

INABILITY OF THE ELASTIC-LAYERED THEORY TO PREDICT PAVEMENT VERTICAL STRESSES

Amara Loulizi
Research Scientist
Virginia Tech Transportation Institute
3500 Transportation Research Plaza
Virginia Tech, Blacksburg, VA 24061-0536
Tel: 540 231-1504, Fax: 540 231-1555
e-mail: amlouliz@vt.edu

Imad L. Al-Qadi
Charles E. Via, Jr. Professor of Civil and Environmental Engineering
200 Patton Hall
Virginia Tech, Blacksburg, VA 24061-0105
Tel: 540 231-5262, Fax: 540 231-7532
e-mail: alqadi@vt.edu

Keywords: Instrumentation, elastic theory, flexible pavements, vertical stress
Word Count: 2477 + 8 figures + 2 Tables = 4977

**Virginia Tech Transportation Institute
Virginia Tech
Blacksburg, Virginia**

ABSTRACT

Since 2000, truck testing has been conducted over the 12 flexible pavement sections of the Virginia Smart Road. The testing has utilized different axle loadings, tire inflation pressures, and speeds under different environmental conditions. Measured collected data include stresses under the pavement layers, horizontal and longitudinal strains under the hot-mix asphalt (HMA) layers, and temperatures at different depths in the pavement system. Vertical stresses were measured in layers of four flexible pavement designs (Sections E, F, G, and H). Sections E and F were built using the same materials, but they have different HMA layer thicknesses. Section G differs from Section F by a 50-mm fine-mix placed underneath the HMA base layer. In addition, Section H has the same structure as Section G, with the exception of a 75mm asphalt treated open-graded drainage layer (OGDL) placed under the HMA base layer. The measured vertical stresses, at different temperatures, underneath the HMA of the aforementioned four sections were compared to those calculated using linear layered elastic theory to identify the conditions under which the theory can be used. Results indicated that the calculated values are higher than those measured at low and intermediate temperatures (approximately $<35^{\circ}\text{C}$). However, at high temperatures (approximately $>35^{\circ}\text{C}$), the layered elastic theory underestimates the vertical stresses significantly.

INTRODUCTION

With the move towards a mechanistic approach for pavement design, accurate determination of the pavement response to truck loading is essential. The 2002 AASHTO design guide proposes the use of elastic layered theory as the backbone of its pavement response model to calculate stresses, strains, and displacements for different temperatures at the critical locations within the pavement structure. The calculated mechanical responses are proposed to be utilized in different performance models to predict distress progression over time. Therefore, an error in the calculated responses would result in an inaccurate life prediction of the pavement.

The layered elastic theory is the tool most often used to calculate flexible pavement response to truck loading; this is due to its simplicity and the fact that pavement engineers have been exposed to it since the 1940s. In 1943, Burmister developed a closed-form solution for a two-layered linearly elastic half-space problem, which was later extended to a three-layer system (1, 2). Since then, and with the advances in computer technology, the theory has been extended to deal with multilayer systems, and a large number of computer programs have been developed accordingly. The major assumptions of the layered elastic theory are the following (3): (1) each layer is assumed homogeneous, isotropic, and linear elastic; (2) all materials are weightless (no inertia effect is considered); (3) all layers are assumed to be infinite in lateral extent; (4) all layers have a finite thickness except for the subgrade, which is assumed to be infinite; (5) pavement systems are loaded statically over a uniform circular area; and (6) the compatibility of strains and stresses is assumed to be satisfied at all layer interfaces.

To assess the accuracy of the elastic layered theory in predicting vertical compressive stresses in flexible pavements, data collected from truck testing conducted on four sections of the Virginia Smart Road Test Facility (4), under different temperatures, were analyzed and compared to calculated values obtained using a layered-elastic theory software. Two types of loadings were considered in this analysis: a single tire with a load of 25.8kN (5.8kips) and a tire inflation pressure of 724kPa (105psi); and a set of dual tires with a load of 39.5kN (8.9kips) and a tire inflation pressure of 724kPa (105psi). All calculations were performed using Kenpave software

developed by Huang (3). This software allows the use of linear elastic, nonlinear, and viscoelastic properties of the materials for the different layers. The software can handle up to 19 layers and performs damage analysis. The interface between the different layers can be specified as either unbonded or fully-bonded.

Vertical compressive stresses were measured in the field using pressure cells, while temperature in the HMA layer was measured using thermocouples. Pressure cells and thermocouples were embedded in the pavement sections during construction. Since the field measured values are considered as the ground-truth values, extreme care was taken to ensure proper data collection and processing (4). This was accomplished through a thorough calibration and installation procedure of the instruments. Repeatability was also insured by placing three instruments per layer and by running a specific test (same speed, same load, and same tire inflation pressure) ten times.

PRESSURE CELLS AND THERMOCOUPLES

Two types of pressure cells were selected. The pressure cells placed in the upper layers of the pavement structure have a diameter of 150mm (6in) and can measure up to 690kPa (100psi). They have been specially designed to withstand high temperatures during the HMA lay-down. The wires used are also for direct burial and can withstand a temperature up to 200°C (392°F). The pressure cells placed in base layers and subgrade have a 225mm (9in) diameter and can measure up to 414kPa (60psi).

Calibration curves were developed by the manufacturer to convert the measured voltage from the pressure cell to pressure. The manufacturer calibration procedure consisted of placing each pressure cell between two rigid plates, which had inflatable rubber membranes. The pressure in these membranes was gradually increased and held constant for a specific time, and then the voltage was measured. This process was repeated until the full range of the pressure cell was covered. To evaluate the manufacturer calibration curves, testing was performed at Virginia Tech using first a Gyratory compactor, then a servo-hydraulic machine. Small differences were found between the manufacturer calibration curves and those obtained using the Gyratory compactor. This difference diminishes at high pressure values. At low pressure, the difference is considered significant due to the edge effect and contact areas between the puck and the pressure cell. Therefore, another test was needed to verify the manufacturer calibration curves.

The pressure cells were then tested using a servo-hydraulic machine. This machine can apply a constant rate of loading and unloading. The pressure cells were evaluated under a combination of different metal loading plate sizes, different layers of rubber membrane placed between the pressure cells and the loading plates, and different loading rates. Figure 1 shows typical responses from a pressure cell at different loading rates and the manufacturer calibration curve (solid line). It was concluded that the relationship between the pressure cell output voltage and the applied pressure is linear and independent of loading rate, and that the calibration curves provided by the manufacturer were acceptable. Pressure cells were carefully installed during construction (Figure 2) and were checked for response immediately after installation.

T-type thermocouple wires (constantan and copper) were used to measure temperature. After fabrication, the response from the thermocouples was checked at two reference temperatures: 0 and 100°C (32 and 212°F). The thermocouples yielded acceptable results.

PAVEMENT DESIGN AND MATERIAL CHARACTERIZATION

Schematic profiles of the four sections used in this study are presented in Figure 3. For Section E, the wearing surface is composed of 38mm (1.5in) of SM-9.5D HMA. In accordance with the Virginia Department of Transportation (VDOT) specifications (5), SM stands for surface mix, 9.5 represents the maximum nominal aggregate size in mm, and the letter D designates the binder type (PG70-22). Under the wearing surface, 225mm (9in) of BM-25.0 HMA base mix is used; BM stands for base mix, and 25.0 stands for the maximum nominal aggregate size in mm. PG64-22 binder is used for this mix. The BM-25.0 is placed above a 150mm (6in) layer of 21-A cement-stabilized aggregate. This layer is supported by a 75mm (3in) layer of 21-B aggregate (8). Section F is similar to Section E; however, the BM-25.0 layer thickness is 150mm (6in) and the 21-B aggregate layer thickness is 150mm (6in). Sections G and F are similar; however, a 50mm layer of a fine surface mix (SM-9.5A; A stands for PG64-22 binder) was used at the bottom of the 100mm-layer of BM-25.0 in Section G. For Section H, a 75mm-layer of an open-graded-drainage-layer (OGDL) was used on top of the 21-A stabilized layer when compared to Section G; and the thickness of the 21-B aggregate layer was reduced to 75mm (3in). The subgrade for all four sections is a fill material composed mainly of rocks and a leveling course of 21-B aggregate.

A series of laboratory and field tests were performed for each material during and after construction of the road. Field testing included density measurements, periodic Falling Weight Deflectometer (FWD) testing, and ground penetrating radar (GPR) surveys.

Table 1 shows the gradation specification for the 21-A and 21-B aggregates. The aggregate gradation of the asphalt treated OGDL is shown in Table 2. Two percent stabilizing binder was used in the mix (PG70-22). Table 2 also shows the aggregate gradation as well as the binder content and type used for all HMA layers.

To analyze the pavement using elastic theory, two material properties were needed for each layer, namely resilient modulus and Poisson's ratio. The resilient modulus of the subgrade, 21-B unbound aggregate, and OGDL, were taken as 330MPa (48ksi), 207MPa (30ksi), and 1400MPa (200ksi), respectively. All these values were obtained from backcalculation of FWD data (6). A Poisson's ratio of 0.45 was assumed for these materials. Based on correlation charts between the unconfined 7-day compressive strength of the 21-A cement stabilized material and the resilient modulus (3), an approximate value of 3580MPa (520ksi) was considered for the resilient modulus of this material. A 0.15 Poisson's ratio was assumed for the 21-A cement stabilized material. The properties of the subgrade, 21-B unbound aggregate, 21-A cement stabilized aggregate, and OGDL were kept constant over temperature. On the other hand, the resilient modulus of the HMA was varied with temperature. Field specimens cored from the four sections, close to where the instruments were placed, were tested in the laboratory for their resilient modulus values at three different temperatures (5°C [41°F], 25°C [77°F], and 40°C [104°F]), as shown in Figure 4. The exponential regression equation was then used to determine the resilient modulus of the HMA at temperatures from 0°C (32°F) to 40°C (104°F), with a 5°C (8°F) increment. Therefore, for each loading, nine runs of the Kenpave software were performed, each at a 5°C (8°F) increment. It should be noted that the SM-9.5D and the BM-25.0 were treated as one HMA layer. The Poisson's ratio of the HMA layer was taken as 0.25 for temperatures below 15°C (59°F), 0.35 for temperatures greater than 15°C (59°F) and less than 30°C (86°F), and 0.45 for temperatures above 30°C (86°F).

RESULTS

Figure 5a shows the measured and calculated vertical compressive stress for Section E under the BM-25.0 layer induced by the 25.8kN (5.8kips) single load. The coefficient of determination, R^2 , value for the measured data regression relationship is approximately equal to 0.9. The measured data also represents truck speeds ranging from 8km/h (5mi/h) to 72km/h (45mi/h); the measured vertical compressive stress is not affected by traveling speed (7). The calculated vertical compressive stress under the BM-25.0 layer was found to vary linearly with temperature, as shown by Equation 2.

$$\sigma_{\text{BM-25.0_Measured}} \text{ (in kPa)} = 3.3e^{0.1T} \quad (1)$$

$$\sigma_{\text{BM-25.0_Calculated}} \text{ (in kPa)} = 62.2 + 1.8T \quad (2)$$

The calculated vertical compressive stress was found to be higher than the measured one for temperatures below approximately 35°C (95°F), after which the measured one becomes higher. Similar results were found for the 39.5kN (8.9kips) dual load as shown in Figure 6b. The equations found for the measured and calculated responses are represented by Equations 3 and 4.

$$\sigma_{\text{BM-25.0_Measured}} \text{ (in kPa)} = 3.6e^{0.09T} \quad (3)$$

$$\sigma_{\text{BM-25.0_Calculated}} \text{ (in kPa)} = 57.0 + 1.4T \quad (4)$$

Figures 6 through 8 show the results for sections F, G, and H, respectively, which are similar to that of E. Also, it is interesting to note, from Figures 7 and 8, that the cutoff temperature where the elastic theory starts to underestimate the measured vertical compressive stress in the HMA layer decreases at locations near the pavement surface. In fact, for these two sections, the cutoff temperature for the vertical compressive stress under the BM-25.0 layer (138mm [5.5in] under the surface) was found to be around 30°C (86°F), while the cutoff temperature for the vertical compressive stress under the SM-9.5A layer (188mm [7.5in] under the surface) was found to be around 35°C (95°F).

CONCLUSIONS AND RECOMMENDATIONS

Testing at the Virginia Smart Road allowed several hypotheses related to flexible-pavement design to be verified. The following findings and recommendations are presented:

1. Results from two loading cases and four different flexible pavement design sections showed that the layered elastic theory overestimates the vertical compressive stress in the flexible pavement layers at low and intermediate temperatures, but it underestimates it at high temperatures.
2. Given that the purpose of a mechanistic pavement design approach is to accurately predict the pavement performance over time, the tool used to calculate stresses, strains, and displacements induced by truck loading in the flexible pavement structure should give close results to those that the pavement will actually encounter. If this tool is not accurate and gives results that are far from the actually field values, the validity of the approach becomes questionable. It is, therefore, recommended that more theoretical modeling using the finite element method (e.g., varying material properties, varying bonding between layers, considering anisotropic properties, dynamic loading, etc.) be performed to achieve a reasonable comparison between measured responses and predicted theoretical responses. Once a theory is validated, predictions of stresses and

strains could be performed for any flexible-pavement design during any period of the year. A follow-up paper to that effect is included in these proceedings (8).

ACKNOWLEDGEMENTS

This research is sponsored by the Virginia Transportation Research Council and the Virginia Department of Transportation. The help of S. Lahouar, W. Nassar, M. El-Seifi, K. Siegel, S. Katicha, A. Appea, B. Diefenderfer, G. Flintsch of Virginia Tech, and the Virginia Department of Transportation personnel D. Clark, K. Taylor, and R. Orren, is greatly appreciated.

REFERENCES

1. Burmister, D. M. The Theory of Stresses and Displacements in Layered Systems and Applications to the Design of Airport runways. *Highway Research Board*, Vol. 23, pp. 126-144, 1943.
2. Burmister, D. M. The General Theory of Stresses and Displacements in Layered Soil Systems. *Journal of Applied Physics*, Vol. 16, pp. 84-94, 1945.
3. Huang, H. Y. *Pavement Analysis and Design*, Prentice Hall, Upper Saddle River, NJ, 1993.
4. Al-Qadi, I.L., A. Loulizi, M.A., Elseifi, and S. Lahouar. The Virginia Smart Road: The Impact of Pavement Instrumentation on Understanding Pavement Performance. *Journal of the Association of Asphalt Pavement Technologists*, Vol. 73, 2004.
5. Virginia Department of Transportation, *Road and Bridge Specification*, Richmond, VA, 2002.
6. Appea, A. K., Validation of FWD Testing Results at the Virginia Smart Road: Theoretically and by Instrument Response, PhD dissertation, Virginia Polytechnic Institute and State University, Blacksburg, VA, 2003.
7. Loulizi, A., I. L. Al-Qadi, S. Lahouar, S., and T. E. Freeman. Measurement of Vertical Compressive Stress Pulse in Flexible Pavements and Its Representation for Dynamic Loading Tests. *Transportation Research Record*, No. 1816, pp. 125-136, 2002.
8. Al-Qadi, I. L., M. Elseifi, and P. J. Yoo, In-Situ Validation of Mechanistic Pavement Finite Element Modeling,” Proceedings of the 2nd International Conference on Pavement Accelerated Facilities, Minneapolis, MN, 2004.

LIST OF TABLES AND FIGURES**TABLE 1 Gradation Specification for 21-A and 21-B Aggregates****TABLE 2 Gradation Specifications and Binder Content for OGDL and HMA****FIGURE 1 Typical pressure cell calibration curves.****FIGURE 2 Pressure cells installed at different layers within the pavement sections.****FIGURE 3 Pavement section designs.****FIGURE 4 Laboratory resilient modulus for the BM-25.0 at different temperatures.****FIGURE 5 Measured and calculated vertical compressive stress under the BM-25.0 layer for section E: (a) single load (b) dual load.****FIGURE 6 Measured and calculated vertical compressive stress under the BM-25.0 layer for section F: (a) single load (b) dual load.****FIGURE 7 Measured and calculated vertical compressive stress for section G: (a) single load (b) dual load.****FIGURE 8 Measured and calculated vertical compressive stress for section H: (a) single load (b) dual load.**

TABLE 1 Gradation Specification for 21-A and 21-B Aggregates.

Sieve Material	Size/	Percent finer than sieve opening (mm)					
		50	25.0	9.5	2.0	0.425	0.075
21-A		100	94-100	63-72	32-41	14-24	6-12
21-B		100	85-95	50-69	20-36	9-19	4-7

TABLE 2 Gradation Specifications and Binder Content for OGDL and HMA.

	Percent finer than sieve opening (mm)								Percent Binder
	37.5	25	19	12.5	9.5	4.75	2.36	0.075	Type
OGDL	100	95		35		7	4	2	2.0% PG70-22
BM-25.0	100	90	83				30	4.5	4.6% PG64-22
SM-9.5D				100	92	53	36	6	5.6% PG70-22
SM-9.5A				100	90	56	34	6	5.6% PG64-22

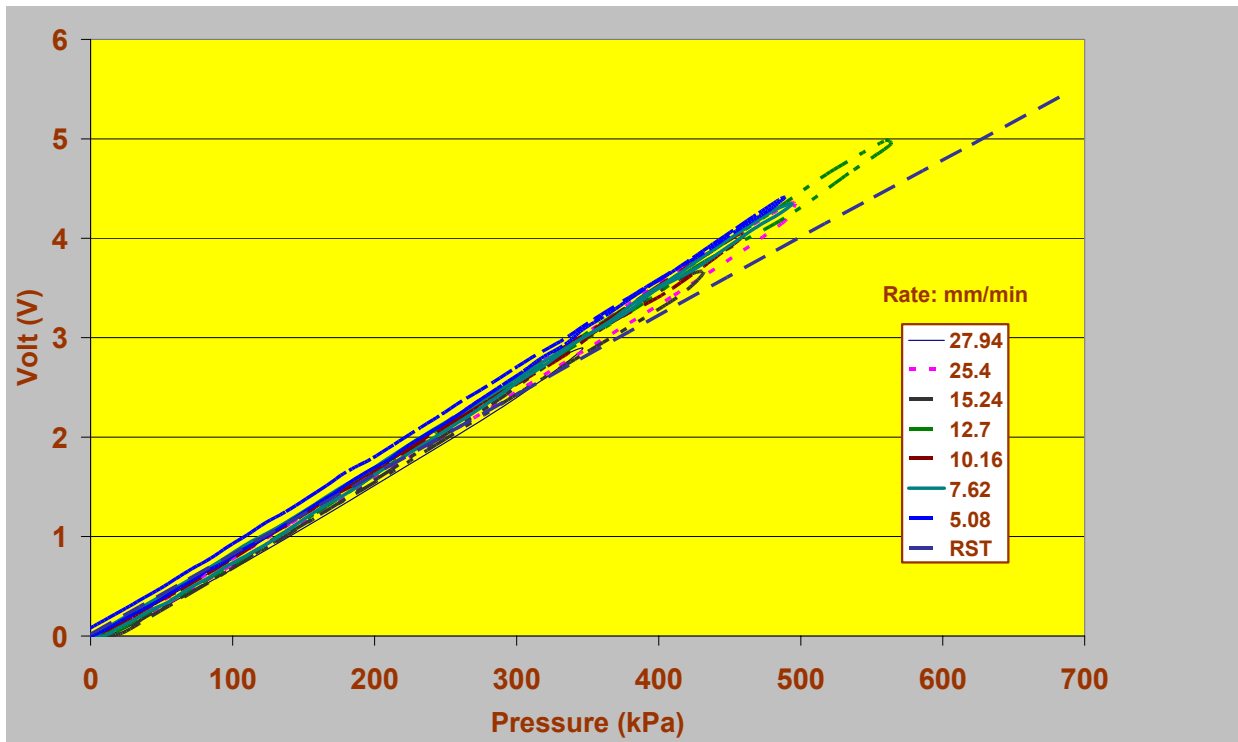


FIGURE 1 Typical pressure cell calibration curves.



FIGURE 2 Pressure cells installed at different layers within the pavement sections.

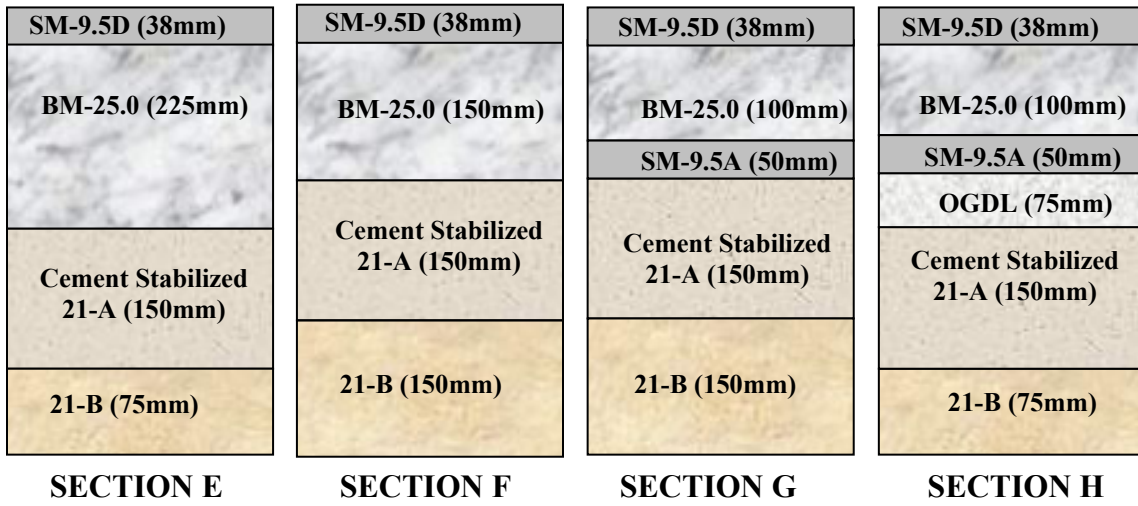


FIGURE 3 Schematic of the pavement section designs.

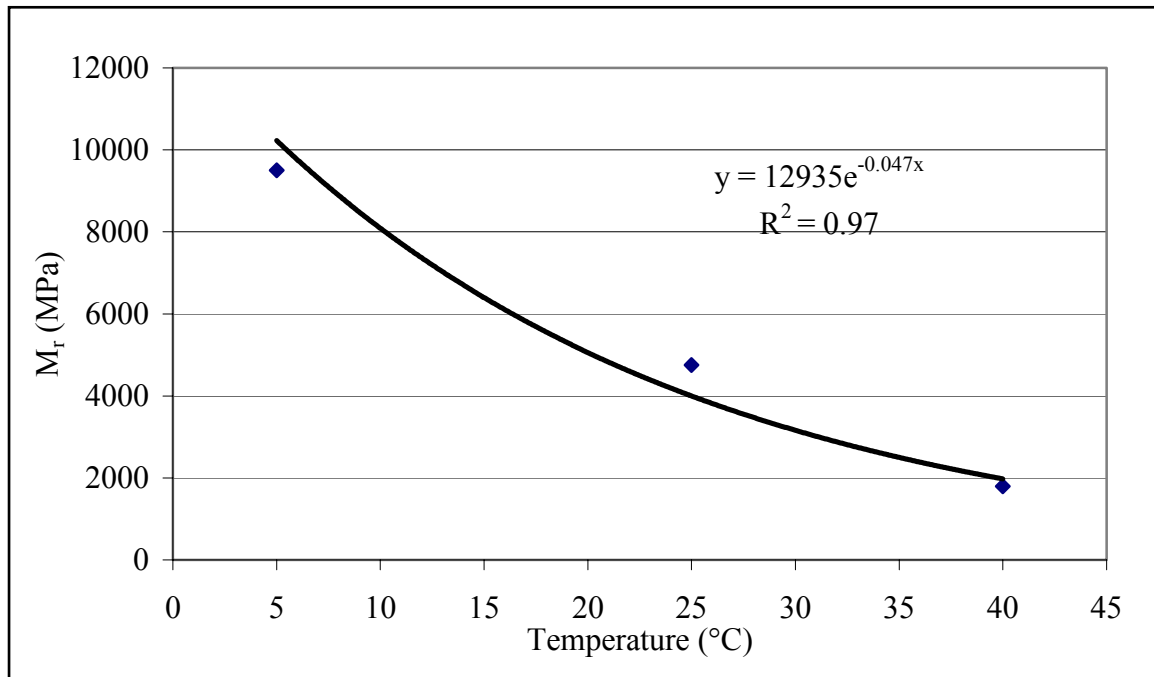
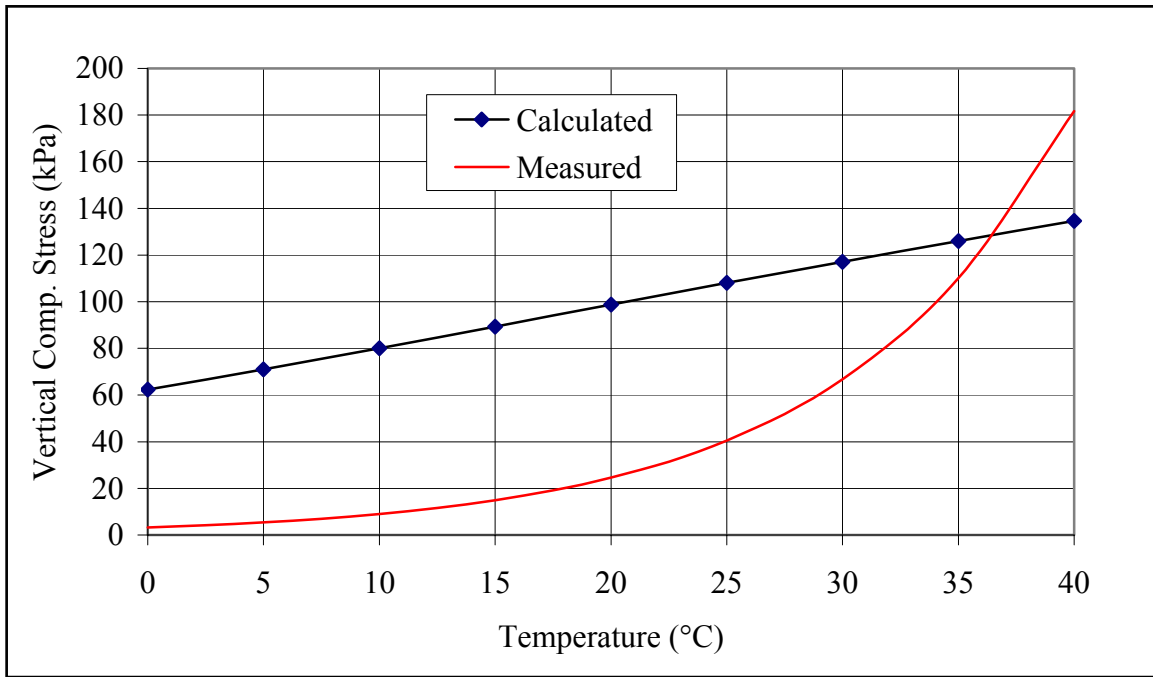
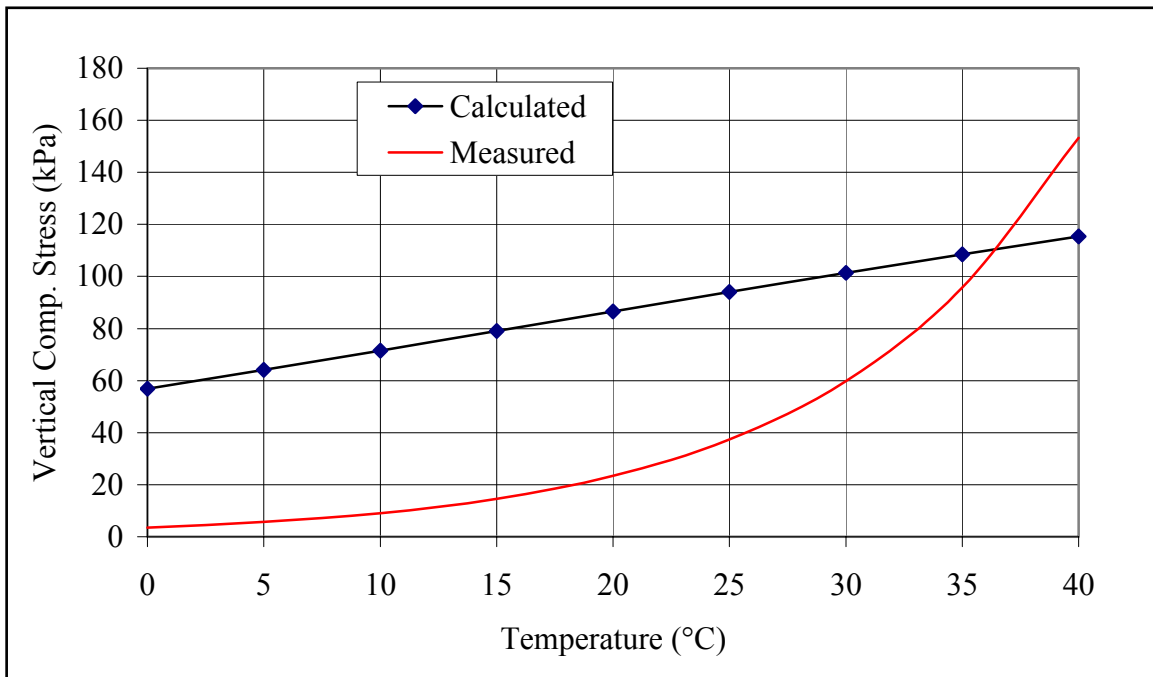


FIGURE 4 Laboratory resilient modulus for the BM-25.0 at different temperatures.

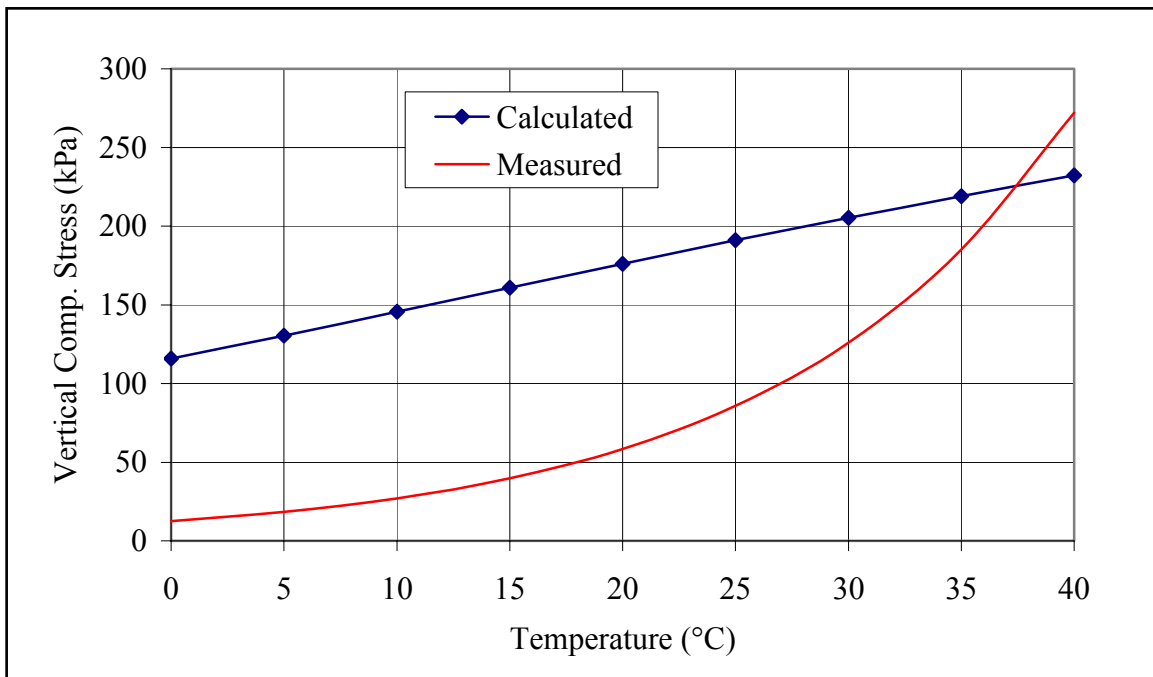


(a)

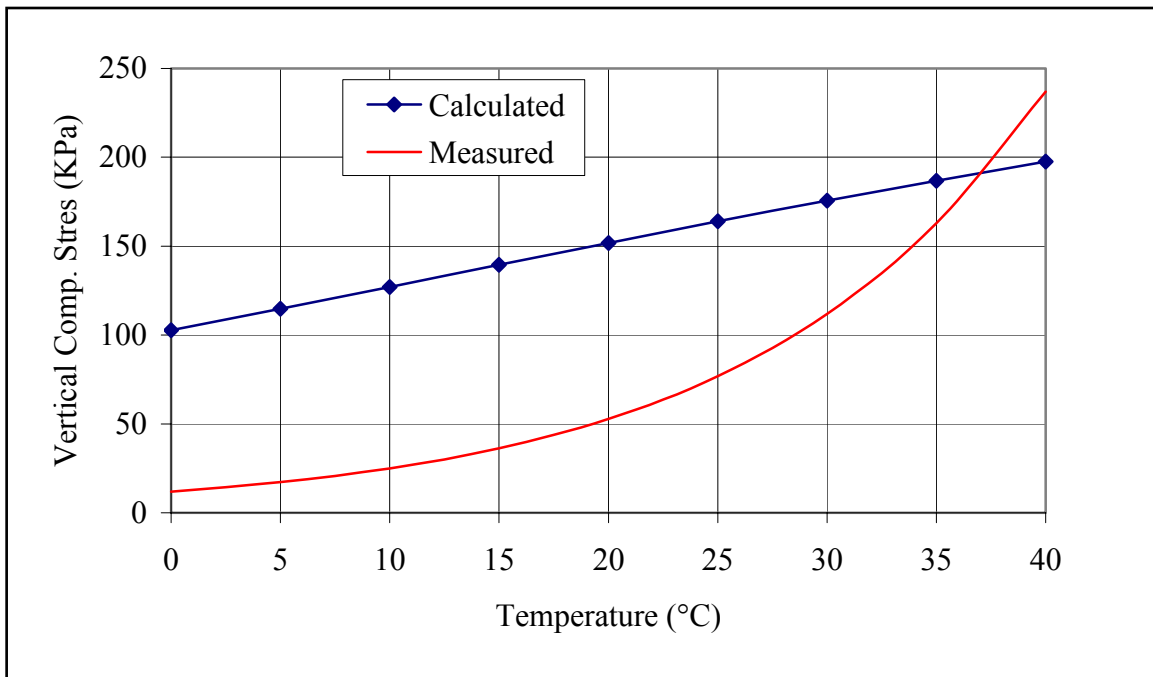


(b)

FIGURE 5 Measured and calculated vertical compressive stress under the BM-25.0 layer for section E: (a) single load (b) dual load.

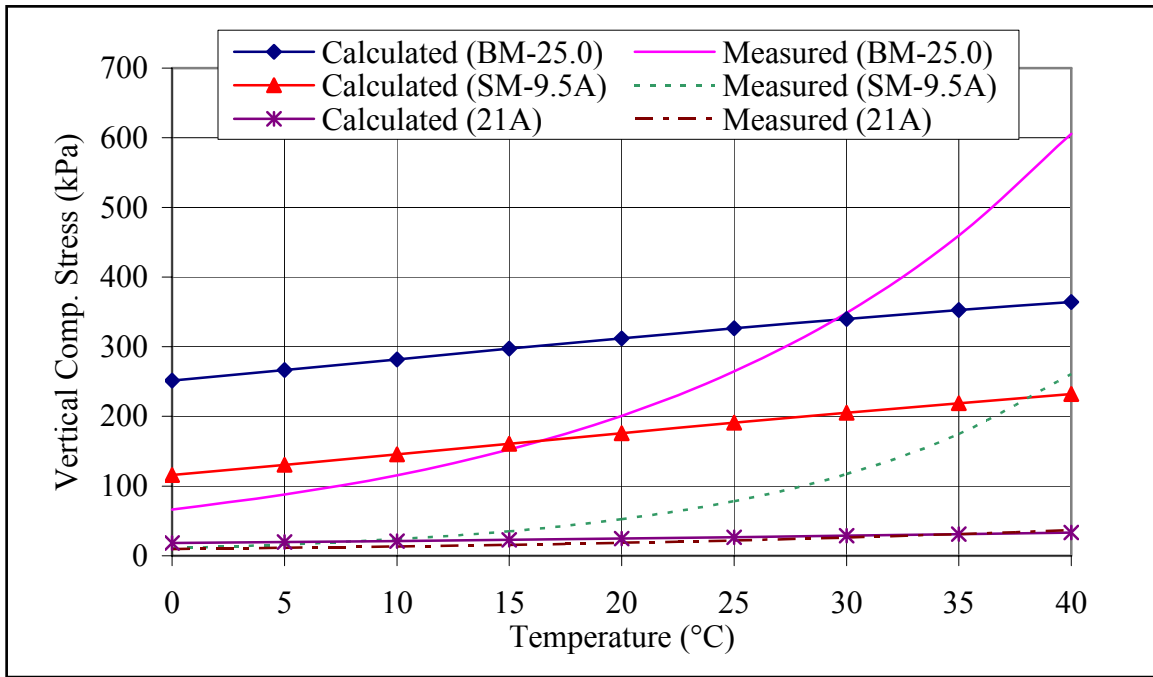


(a)

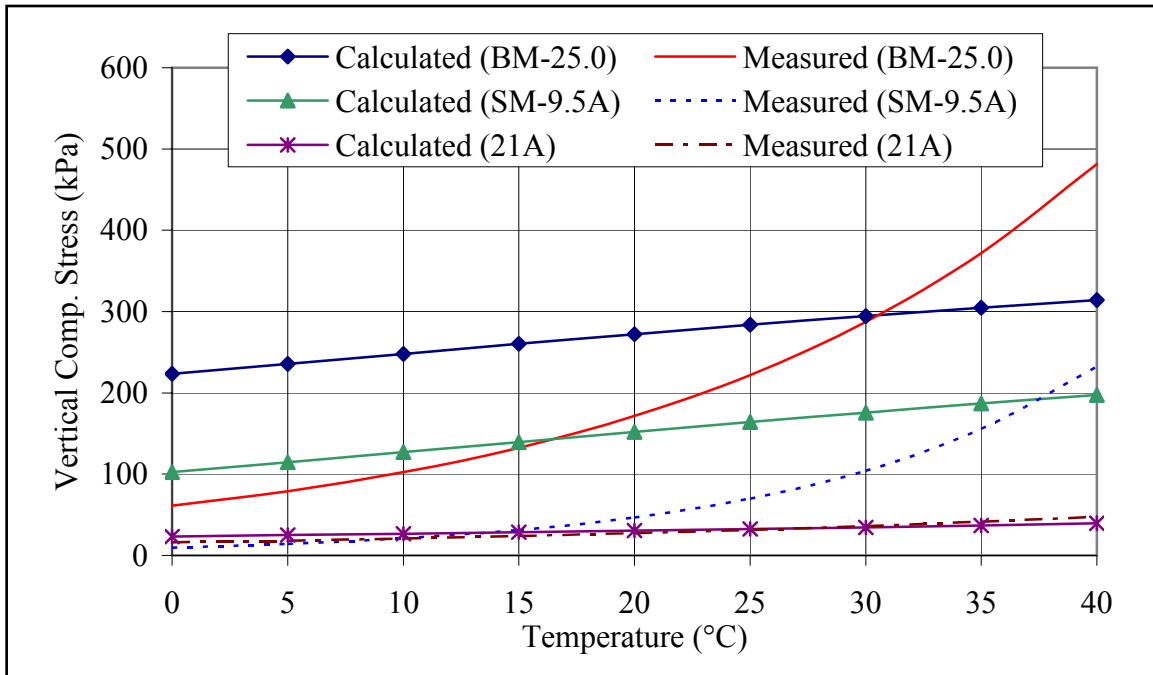


(b)

FIGURE 6 Measured and calculated vertical compressive stress under the BM-25.0 layer for section F: (a) single load (b) dual load.

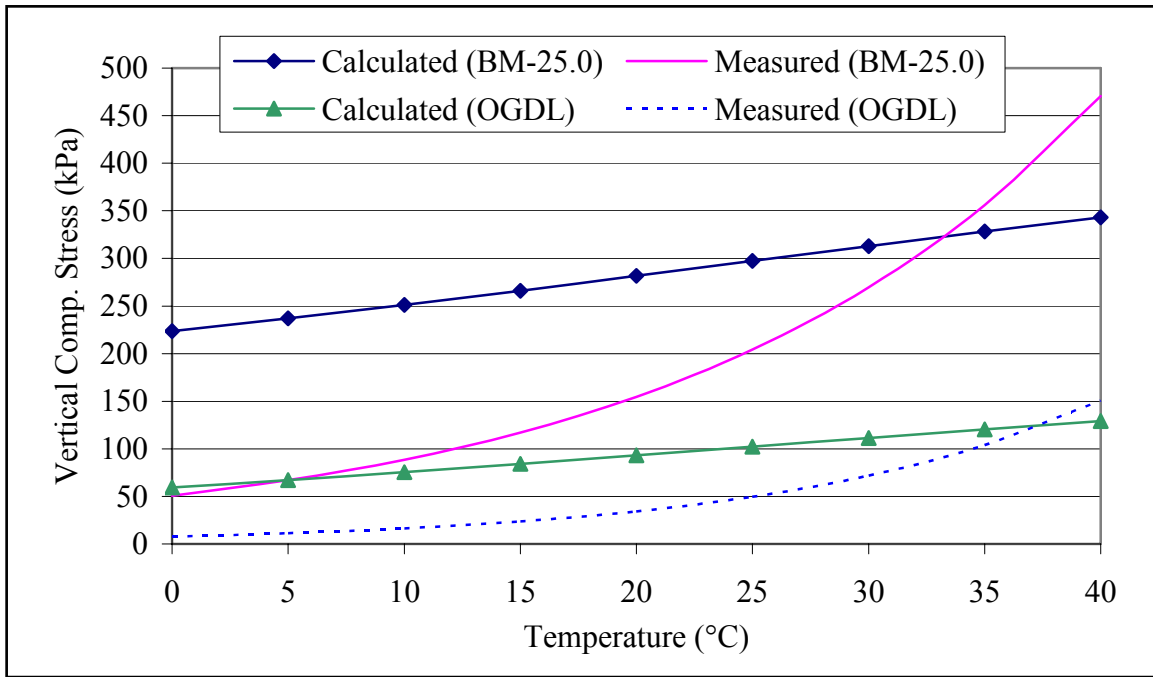


(a)

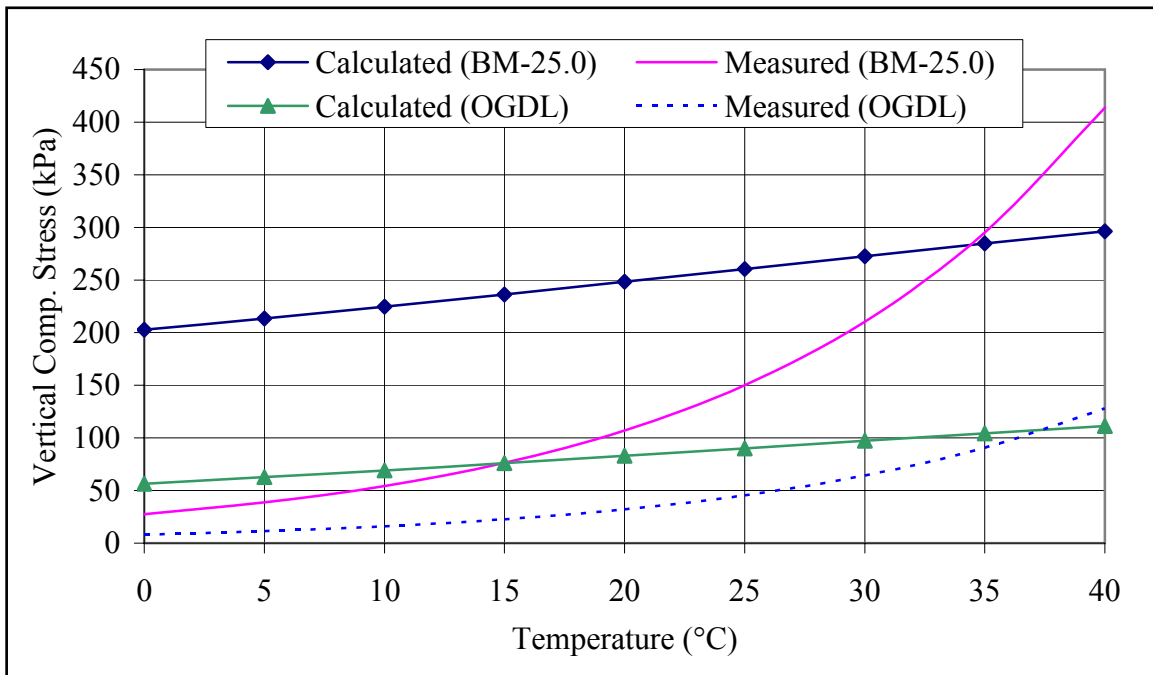


(b)

FIGURE 7 Measured and calculated vertical compressive stress for section G: (a) single load (b) dual load.



(a)



(b)

FIGURE 8 Measured and calculated vertical compressive stress for section H: (a) single load (b) dual load.